

DETERMINATION OF STELLAR ELLIPTICITIES IN FUTURE MICROLENSING SURVEYS

CHEONGHO HAN

Department of Physics, Institute for Basic Science Research, Chungbuk National University, Chongju 361-763, Korea;
cheongho@astroph.chungbuk.ac.kr

AND

HEON-YOUNG CHANG

Department of Astronomy and Atmospheric Sciences, Kyungpook National University, 1370 Sankyuk-dong, Buk-gu, Daegu 702-701, Korea;
hyc@knu.ac.kr

Draft version May 13, 2018

ABSTRACT

We propose a method that can determine the ellipticities of source stars of microlensing events produced by binary lenses. The method is based on the fact that the products of the caustic-crossing timescale, Δt , and the cosine of the caustic incidence angle of the source trajectory, κ , of the individual caustic crossings are different for events involving an elliptical source, while the products are the same for events associated with a circular source. The product $\Delta t_{\perp} = \Delta t \cos \kappa$ corresponds to the caustic-crossing timescale when the incidence angle of the source trajectory is $\kappa = 0$. For the unique determination of the source ellipticity, resolutions of at least three caustic crossings are required. Although this requirement is difficult to achieve under the current observational setup based on alert/follow-up mode, it will be possible with the advent of future lensing experiments that will survey wide fields continuously at high cadence. For typical Galactic bulge events, the difference in Δt_{\perp} between caustic crossings is of the order of minutes depending on the source orientations and ellipticities. Considering the monitoring frequency of the future lensing surveys of ~ 6 times/hr and the improved photometry especially of the proposed space-based survey, we predict that ellipticity determinations by the proposed method will be possible for a significant fraction of multiple caustic-crossing binary lens events involving source stars having non-negligible ellipticities.

Subject headings: gravitational lensing – stars: fundamental parameters

1. INTRODUCTION

Microlensing was originally proposed to search for Galactic dark matter in the form of massive compact halo objects (Paczynski 1986). However, with the ability to detect a large number of events, especially toward the Galactic bulge field, and to intensively monitor the detected events from follow-up observations, microlensing has been developed into a powerful tool to study various aspects of stellar astrophysics (Gould 2001). Especially, intensive observations of caustic-crossing binary lens events make it possible to measure the limb-darkening structure of stars, which in essence maps the atmospheric temperature as a function of depth.

Recently, Rattenbury et al. (2005) demonstrated an additional applicability of microlensing in stellar astrophysics by measuring the shape of the source star in microlensing event MOA 2002-BLG-33. Due to rotation, stars are not exactly circular. For example, Altair (α Aquillae) has an ellipticity of $e = (1 - b^2/a^2)^{1/2} = 0.23$ (van Belle 2001) and the Achernar (α Eridani), the flattest star ever measured, has an ellipticity of $e = 0.59$ (Domiciano de Souza et al. 2003). The star measured by Rattenbury et al. (2005) has an ellipticity of $e = 0.2$. Here a and b represent the angular sizes of the semi-major and semi-minor axes, respectively. The nature of the source flattening makes the lensing lightcurve differ from that of a circular case. However, detecting the deviation induced by the source flattening is very difficult because the deviation is much smaller than the deviation caused by limb darkening (see § 3). For the case of MOA 2002-BLG-33, an ellipticity measurement was possible because of the very special lens-source geometry in which the source star was closely bounded on all sides by the caustics of the lens. However, such a case is extremely rare.

In this paper, we propose a more general method that can determine the source ellipticity. The method requires to resolve at least three caustic crossings and precisely measure the durations of the individual caustic crossings. Although this requirement is difficult to achieve under the current observational setup based on alert/follow-up, it can be achieved by future lensing experiments that can survey wide fields continuously at high cadence.

The paper is organized as follows. In § 2, we describe the basics of caustic-crossing binary lens events involving elliptical source stars. In § 3, we demonstrate the difficulties in noticing the elliptical nature of source stars from the lightcurve of a single caustic crossing. In § 4, we explain how the source ellipticity is measured by the proposed method and demonstrate the feasibility of the method. In § 5, we summarize the results and conclude.

2. CAUSTIC CROSSING OF AN ELLIPTICAL SOURCE

If a microlensing event is caused by a lens system composed of two masses, the resulting lightcurve can differ dramatically from the smooth and symmetric curve of a single lens event. The main new feature of binary lensing is the caustics, which represent the positions in the source plane where the lensing magnification of a point source becomes infinite. The set of caustics forms one or multiple closed figures where each figure is composed of concave line segments (fold caustics) that meet at points (cusps). The number of separate sets of caustics is unity when the separation between the lens components is comparable to the Einstein ring radius θ_E , and it becomes two and three when the separation is substantially larger and smaller than θ_E , respectively. Due to the larger cross-section of the fold caustic compared to the cusp, major-

ity of caustic crossing events are fold-caustic crossings. Near a fold caustic, the magnification of the source star brightness is $A \propto u_{\perp}^{-1/2}$, where u_{\perp} is the angular normal distance of the source from the fold caustic in units of the Einstein ring radius. Because of the divergent nature of the lensing magnification near the caustic, i.e. $A \rightarrow \infty$ as $u_{\perp} \rightarrow 0$, the lightcurve of a caustic-crossing event is characterized by sharp spikes. Since the caustics form closed figures, caustic crossings occur in multiple times of two (at the entrance and exit of the caustic). Mao & Paczyński (1991) predicted that $\sim 7\%$ of all Galactic microlensing events would be caustic-crossing events and this rate is roughly consistent with that detected by the MACHO (Alcock et al. 2000) and OGLE (Jaroszyński 2002) lensing surveys.

The usefulness of caustic-crossing events lies in the divergent nature and large gradient of the lensing magnification near the caustic. When a source approaches the caustic, different parts of the source star surface are magnified by different amounts (finite-source effect). Then, the lensing magnification of a finite source is equivalent to the intensity-weighted mean value averaged over the source star surface, i.e.

$$A_{fs}(\zeta) = \frac{\int_S I(\zeta') A(\zeta + \zeta') d\zeta'}{\int_S I(\zeta') d\zeta'}, \quad (1)$$

where A denotes the point-source magnification, ζ is the vector position of the center of the source, ζ' is the displacement vector of a point on the source star surface with respect to the source star's center, $I(\zeta')$ is the intensity profile of the source star, and the two-dimensional integral is over the source-star surface S . Precise photometry during the caustic crossing enables one to measure the limb-darkening profiles of source stars (Witt 1995) and the limb-darkening coefficients of six stars with various stellar types were actually measure by this method (Albrow et al. 1999a,b, 2000, 2001; Afonso et al. 2000; Fields et al. 2003; Kubas et al. 2005). It is also possible to study irregular structures on the source star surface, such as spots (Han, et al. 2000; Chang & Han 2002; Hendry et al. 2002).

The lensing magnification of a caustic-crossing binary lens event involving a *circular* source is characterized by eight parameters. Three of these are identical to those of a single point-lens event: the Einstein timescale, t_E , the time of the closest source approach to the center of the binary lens system, t_0 , and the separation between the source and center at that time, u_0 . For a binary lens, the lensing magnification is not radially symmetric and thus an additional parameter of the angle between the source trajectory and the binary axis, α , is required to characterize the source trajectory. Another two are the parameters related to the binary lens system: the mass ratio, q , and the separation (normalized by θ_E), s , between the lens components. The final two parameters are related to the source star: the normalized source radius, $\rho_* = \theta_*/\theta_E$, and the limb-darkening coefficient. Here θ_* represents the angular radius of the source star. For a limb-darkened source, the surface brightness profile is often modeled as

$$\frac{I(\theta)}{I(0)} = 1 - \Gamma_{\lambda} \left[1 - \frac{3}{2} \sqrt{1 - \left(\frac{\theta}{\theta_*} \right)^2} \right], \quad (2)$$

where Γ_{λ} is the limb-darkening parameter and θ is the angular distance measured on the source star surface from the center to the position within the source. In the standard formalism,

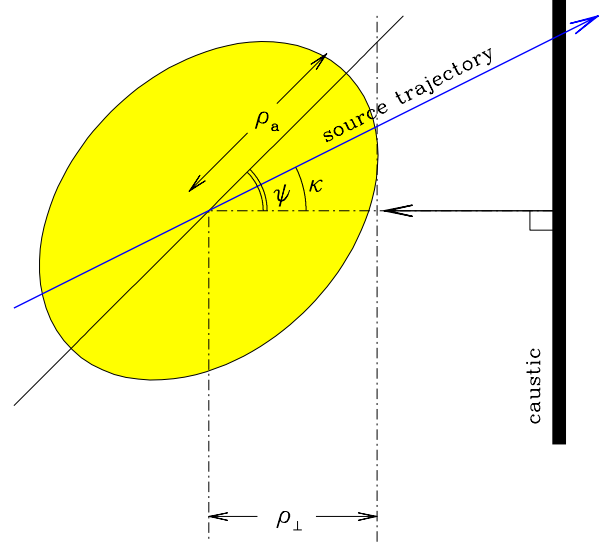


FIG. 1.— Definitions of the source orientation angle ψ , caustic incidence angle κ , normalized semi-major axis ρ_a , and the projected width ρ_{\perp} of the source star.

the linear limb darkening is expressed as

$$\frac{I(\theta)}{I(0)} = 1 - c_{\lambda} \left[1 - \sqrt{1 - \left(\frac{\theta}{\theta_*} \right)^2} \right]. \quad (3)$$

Then, the relationship between the expressions of the linear limb-darkening coefficients is

$$c_{\lambda} = \frac{3\Gamma_{\lambda}}{\Gamma_{\lambda} + 2}. \quad (4)$$

For an event involving an *elliptical* source, two additional parameters are needed. These are the eccentricity of the source, e , and the orientation angle of the source major axis with respect to the perpendicular to the caustic, ψ (see Fig. 1). Therefore, the total number of parameters required for the full characterization of a caustic-crossing binary lens event associated with an elliptical source is ten.

3. SINGLE CAUSTIC CROSSING

Due to the intrinsic difference in shape, the lightcurve of a caustic-crossing binary lens event involving an elliptical source differs from that of an event associated with a circular source. However, detecting the deviation induced by the source flattening is difficult. This is in part because the flattening of the majority of stars is small. However, we find that even in the case of severely flattened stars the deviation caused by the source flattening is substantially smaller than the deviation caused by the limb darkening. In this section, we demonstrate this fact.

To see the pattern of deviations induced by the source flattening and compare the magnitude of the deviation to that caused by limb darkening, we simulate events associated with source stars having various shapes, sizes, and limb-darkening coefficients. For the cases of events with circular sources, we consider limb darkening. We test four cases of limb darkening coefficients of $\Gamma_{\lambda} = 0.1, 0.3, 0.5,$ and 0.7 , which cover most values ranging from main-sequence to giant stars. The tested value of the normalized source radius is $\rho_* = 0.02$, which

roughly corresponds a giant source star of a typical Galactic bulge event. For events with elliptical sources, however, we do not consider limb-darkening effect, so as to isolate the magnitude of deviation caused only by source flattening. We test three different elliptical cases where the individual source stars have a common ellipticity but different orientation angles. For the ellipticity, we adopt a relatively large value of $e = 0.5$ ($b/a = 0.866$). The tested values of the orientation angle are $\psi = 0^\circ, 30^\circ, \text{ and } 90^\circ$. We set the normalized semi-major axes, $\rho_a = a/\theta_E$, of the individual elliptical source stars with different orientation angles so that the times of the caustic entrance and exit (and thus the duration of caustic crossing) match those of the circular source case. As a result, the individual elliptical source stars have different semi-major axes with ratios of $\rho_a(\psi = 0^\circ) : \rho_a(\psi = 30^\circ) : \rho_a(\psi = 60^\circ) = 1.000 : 1.035 : 1.110$ (see the top panel of Fig. 2). The duration of caustic crossing is proportional to the projected width of the source star in the direction perpendicular to the caustic, ρ_\perp (projected width, see Fig. 1). The projected width is related to the semi-major axis and orientation angle by

$$\Delta\rho_\perp = \rho_a \left[\frac{(1-e^2)^2 + \cot^2\psi}{1-e^2 + \cot^2\psi} \right]^{1/2}. \quad (5)$$

All lightcurves are produced by the same binary lens system with $q = 0.8$ and $s = 1.2$ and the parameters related to the source trajectory are $u_0 = 0.27$ and $\alpha = 0^\circ$. The angle of the source trajectory with respect to the perpendicular to the caustic, κ (caustic incidence angle, see Fig. 1), is very close to zero.

In Figure 2, we present the results of the simulation where the middle panel shows the magnifications of the individual tested events, A , and the bottom panel shows the deviations from a uniform circular case A_0 . The top panel shows the shapes and orientations of the tested source star. The lightcurves of the limb-darkened circular source cases show a characteristic pattern in which the deviation is negative when the caustic is located on the fainter edge of the source while the deviation is positive when the caustic is positioned on the brighter central part. The elliptical cases show more complex pattern depending on the the size and orientation of the source star. However, regardless of the variation, the deviation induced by the source flattening is substantially smaller than the deviation caused by the limb-darkening effect.

4. MULTIPLE CAUSTIC CROSSINGS

4.1. Basic Scheme of the Method

Although difficult with only a single caustic-crossing lightcurve, it is possible to notice the elliptical nature of the source star if both the entrance and exit of the caustic are well resolved. This is possible because the products of the caustic-crossing timescale and the cosine of the caustic incidence angle, i.e. $\Delta t \cos \kappa$, of the individual caustic crossings are different each other for an elliptical source. For a circular source, on the other hand, the products are always the same regardless of the source orientation. The product corresponds to the caustic-crossing timescale when the incidence angle of the source trajectory is $\kappa = 0^\circ$ (hereafter we refer to the product as the ‘normal incidence caustic-crossing timescale’ and denote as Δt_\perp). The normal incidence caustic-crossing timescale is related to the source parameters by

$$\Delta t_\perp = \Delta t \cos \kappa = 2 \left[\frac{(1-e^2)^2 + \cot^2\psi}{1-e^2 + \cot^2\psi} \right]^{1/2} \rho_a t_E. \quad (6)$$

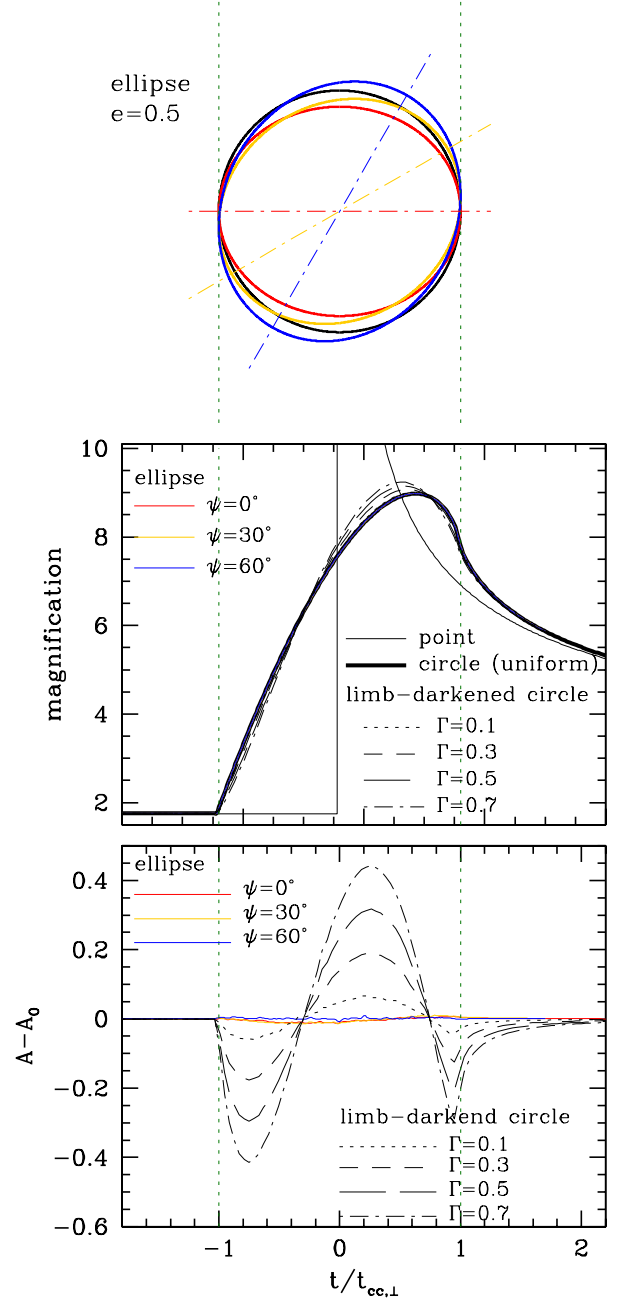


FIG. 2.— Lightcurves of caustic-crossing binary lens events associated with source stars having various shapes, sizes, and limb-darkening coefficients (middle panel) and the deviations from a uniform circular case (bottom panel). Top panel shows the shapes and orientations of tested source stars.

We note that the caustic-crossing timescale Δt is defined as the duration between the source’s enter and exit of the caustic. For each caustic crossing, the caustic-crossing timescale is measured from the lightcurve during the caustic crossing. The incidence angles κ of the individual caustic crossings and the Einstein timescale t_E are determined from the model fit to the overall shape of the lightcurve.

Although the elliptical nature of the source star can be noticed from two caustic crossings, unique determination of the source ellipticity requires an additional crossing. The nor-

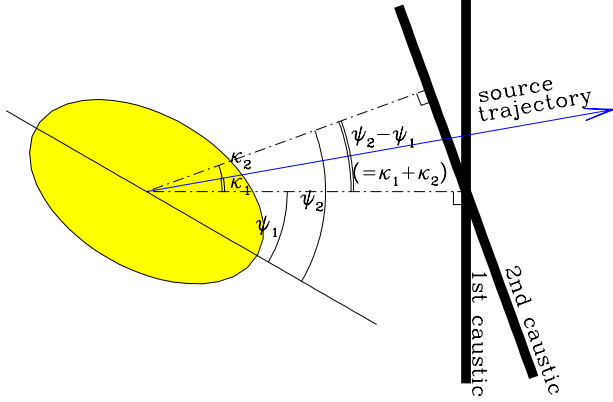


FIG. 3.— Relation between the source orientation angles ψ_1 and ψ_2 with respect to the perpendiculars to first and second caustics. κ_1 and κ_2 are the incidence angles of the source star to the first and second caustics, respectively.

mal incidence caustic-crossing timescale is a function of three unknowns of ρ_a , e , and ψ , i.e. $\Delta t_{\perp} = \Delta t_{\perp}(\rho_a, e, \psi)$. If one resolved the lightcurve profiles of two caustic crossings, the number of measured quantities increases to two, i.e. the normal incidence caustic-crossing timescales at the first and second caustic crossings, $\Delta t_{\perp,1}$ and $\Delta t_{\perp,2}$, but the number of unknowns remains the same. This is because the source orientation angles of the individual caustic crossings are related each other. This is demonstrated in Figure 3. In the presented case, the orientation angle at the second caustic crossing ψ_2 is related to the orientation angle at the first crossing ψ_1 by $\psi_2 = \psi_1 + \kappa_1 + \kappa_2$, where κ_1 and κ_2 are the caustic incidence angles at the first and second caustic crossings, respectively. However, with two caustic crossings, the number of unknowns still exceeds that of measured quantities. Therefore, if one has an additional lightcurve of caustic crossing, the numbers of unknowns and measured quantities become the same, and thus one can uniquely determine all three unknowns of ρ_a , e , and ψ_1 (and subsequently ψ_2 and ψ_3).

There are two channels for multiple caustic crossings. One is the case in which the source trajectory passes two separate sets of caustics. The other channel is the case where the source trajectory is aligned closely along a fold of the caustic as shown in an example in Figure 4. Multiple crossings through the second channel can occur because fold caustics have concave curvature. If the individual caustic crossings of these events are resolved, the events will provide precious chances of measuring the source ellipticities.

4.2. Feasibility of the Method

The basic requirement of the proposed method is resolving multiple caustic crossings. Currently, microlensing follow-up observation is possible only after an alert is issued. Under this strategy, the first caustic crossing is usually missed due to the unpredictable nature and short duration of the caustic crossing. The second caustic crossing may be resolved because the crossing can be roughly predicted from the characteristic ‘‘U’’ shape of the lightcurve when the source is inside the caustic (Jaroszyński & Mao 2001). In addition, there is a guarantee that the second crossing should occur and thus it is worth devoting observational resources for the resolution of the second caustic crossing. However, there is no characteristic pattern

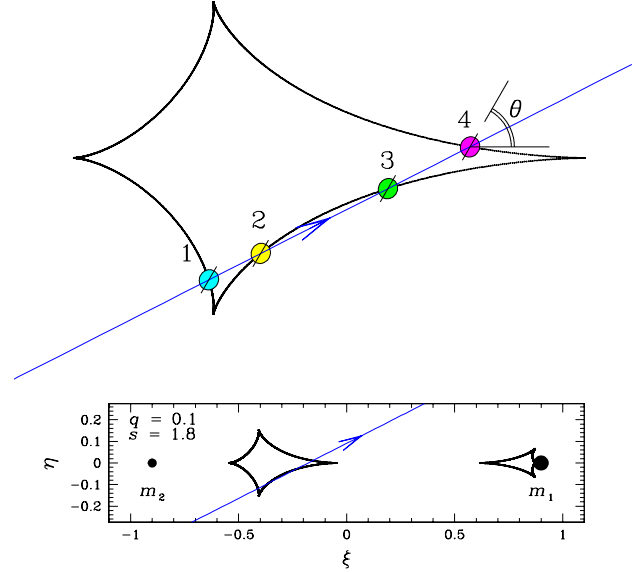


FIG. 4.— An example event with multiple caustic crossings. The small ellipses on the source trajectory (straight line with an arrow) represent the source star at the times of the caustic crossings, which are numbered according to the order of time. The size and flattening of the source star are exaggerated to better show the orientations of the major axis. The angle θ is the orientation angle of the source star major axis with respect to the binary axis. The small bottom panel shows the lens system geometry, where the positions of the lens components (m_1 and m_2), caustics, and source trajectory are marked.

between the pairs of the caustic crossings, and thus it would be difficult to predict when the additional crossings will occur. Furthermore, there is no guarantee that these additional crossings will occur. Therefore, considering that the main object of the follow-up observation is detecting deviations induced by planetary companions, it would be difficult to devote the limited resources waiting for unpredictable additional caustic crossings.

However, the limitation can be overcome with the advent of future lensing experiments that can survey wide fields continuously at high cadence by using very large format cameras. Two such surveys were proposed. The *Galactic Exoplanet Survey Telescope (GEST)*, whose concept was succeeded by the *Microlensing Planet Finder (MPF)*, is a space mission to be equipped with a 1.0m – 1.5m telescope (Bennett & Rhie 2002). The ‘Earth Hunter’ project plans to achieve high monitoring frequency by using three 2m-class wide-field ground-based telescopes scattered over the southern hemisphere (A. Gould, private communication). These next-generation surveys will dispense with the alert/follow-up mode and instead simultaneously obtain densely sampled lightcurves of all microlensing events in the field. These experiments are expected to detect of order 5000 events per year. Therefore, the set of multiple caustic-crossing events for which an ellipticity measurement is possible would not be vanishingly small.

To investigate the feasibility of implementing the proposed method in future lensing surveys, we estimate the magnitude of the difference in the normal incidence caustic-crossing timescales between caustic crossings, $\Delta t_{\perp,i} - \Delta t_{\perp,j}$, expected from typical Galactic binary lens events. As an example, we choose an event produced by a binary lens system with a mass ratio and separation of $q = 0.1$ and $s = 1.8$, respectively. Fig-

TABLE 1
NORMAL INCIDENCE CAUSTIC-CROSSING TIMESCALES

θ ($^\circ$)	crossing number	κ ($^\circ$)	ψ ($^\circ$)	$e = 0.2$	Δt_{\perp} (hr)				
					$e = 0.3$	$e = 0.4$	$\max \Delta t_{\perp,i} - \Delta t_{\perp,j} $ (hr)		
							$e = 0.2$	$e = 0.3$	$e = 0.4$
30	1	9.718	12.718	1.9182	1.9162	1.9137	0.0359	0.0820	0.1488
	2	77.689	80.689	1.8823	1.8342	1.7649			
	3	80.424	77.424	1.8831	1.8363	1.7691			
	4	53.208	50.208	1.8976	1.8703	1.8339			
60	1	9.718	42.718	1.9026	1.8819	1.8548	0.0293	0.0667	0.1204
	2	77.689	69.311	1.8863	1.8438	1.7839			
	3	80.424	47.424	1.8995	1.8746	1.8418			
	4	53.208	20.208	1.9156	1.9105	1.9042			
90	1	9.718	72.718	1.8848	1.8403	1.7769	0.0341	0.0775	0.1393
	2	77.689	39.311	1.9049	1.8870	1.8638			
	3	80.424	17.424	1.9167	1.9129	1.9082			
	4	53.208	9.792	1.9189	1.9177	1.9162			

Figure 4 shows the caustics and source trajectory of the example event. For the source star, we assume a normalized semi-major axis of $\rho_a = 0.002$, which corresponds to that of a F0 main-sequence source star of a typical Galactic bulge event produced by a low-mass stellar lens with distances to the lens and source of $D_L \sim 6$ kpc and $D_S \sim 8$ kpc. We test three different ellipticities of $e = 0.2, 0.3$, and 0.4 , which correspond to the axis ratios of $b/a = 0.979, 0.954$, and 0.917 , respectively. We test three cases of source orientations where the angles between the source major axis and the binary axis are $\theta = 30^\circ, 60^\circ$, and 90° (see the definition of θ in Fig. 4). The small ellipses on the trajectory in Figure 4 represent the source star at the times of caustic crossings. We designate the individual crossings by numbers according to the order of time. We note that the source star in the figure is bigger and flatter than the actual tested stars to better show the orientations of their major axes.

The results are summarized in Table 1, where we present the crossing number, caustic incidence angle κ , source orientation angle ψ , and the normal incidence caustic-crossing timescales Δt_{\perp} of the individual caustic crossings. Also presented are the maximum values of the differences between the normal incidence caustic-crossing timescales, i.e. $\max|\Delta t_{\perp,i} - \Delta t_{\perp,j}|$. The range of the difference is order of minutes depending on the source orientation and ellipticity.

Then, what would be the precision of Δt measurement? In an ideal case where there are N equally spaced measurements over the caustic crossing with a fractional photometric precision σ , the times of the caustic entrance and exit can be known with a precision of $\sim \sigma \Delta t / \sqrt{N}$. In reality, however, the actual error, $\delta(\Delta t)$ would be larger than this due to various factors. Estimating error in Δt measurement considering all these factors is difficult. We, therefore, estimate the ratio of the actual error to the value of the ideal case, i.e. $f = \delta(\Delta t) / (\sigma \Delta t / \sqrt{N})$, based on the error estimate in actually observed caustic crossings. For this, we choose two events with well resolved caustic crossings of MACHO 98-SMC-1 (Albrow et al. 1999b) and OGLE-1999-BUL-23 (Albrow et al. 2001). Assuming $\sigma = 2\%$, we find that $f \sim 2.7$ and 1.9 for the individual events. By taking $f = 2.0$ as a representative value, we then estimate

the precision of Δt measurement in the next-generation experiments as

$$\delta(\Delta t) \sim f \frac{\sigma \Delta t}{\sqrt{N}}. \quad (7)$$

By assuming a typical caustic crossing timescale of $\Delta t \sim 2$ hrs, the photometric precision of $\sigma \sim 0.5\%$, and the monitoring frequency of 6 times/hr (and thus $N \sim 12$), we find that $\delta(\Delta t) \sim 0.3$ min. Considering that the typical value of the difference $|\Delta t_{\perp,i} - \Delta t_{\perp,j}|$ is order of minutes, we predict that ellipticity measurements will be possible for a significant fraction of multiple caustic-crossing events involving source stars having non-negligible ellipticities.

5. CONCLUSION

We have proposed a method that can determine the ellipticities of source stars of microlensing events produced by binary lenses. The method is based on the fact that the normal incidence caustic-crossing timescales of the individual caustic crossings are different for events involving an elliptical source, while the timescales are the same for events associated with a circular source. For the unique determination of the source ellipticity, resolutions of three and more caustic crossings are required. Although this requirement is difficult to achieve under the current observational setup, it will be possible with the advent of future lensing experiments that will survey wide fields continuously at high cadence. For typical Galactic bulge events, the difference in Δt_{\perp} between caustic crossings is order of minutes. Considering the high monitoring frequency of the future lensing surveys and the improved photometry especially of the proposed space-based survey, we predict that ellipticity determinations by the proposed method will be possible for a non-negligible number of events.

We would like to thank A. Gould for making helpful comments. This work was supported by the Astrophysical Research Center for the Structure and Evolution of the Cosmos (ARCSEC) of the Korea Science & Engineering Foundation (KOSEF) through the Science Research Program (SRC) program.

REFERENCES

Afonso, C., et al. 2000, ApJ, 532, 340
Albrow, M. D., et al. 1999a, ApJ, 522, 1011

Albrow, M. D., et al. 1999b, ApJ, 522, 1022
Albrow, M. D., et al. 2000, ApJ, 534, 894

- Albrow, M. D., et al. 2001, *ApJ*, 549, 759
Alcock, C., et al. 2000, *ApJ*, 532, 340
An, J. H., et al. 2002, *ApJ*, 572, 521
Bennett, D. P., & Rhie, S. H. 2002, *ApJ*, 574, 985
Castro, S., Pogge, R. W., Rich, R. M., DePoy, D. L., & Gould, A. 2001, *ApJ*, 548, L197
Chang, H.-Y., & Han, C. 2002, *MNRAS*, 335, 195
Domiciano de Souza, A., et al. 2003, *A&A*, 407, L47
Fields, D. L., et al. 2003, *ApJ*, 596, 1305
Gould, A. 2001, *PASP*, 113, 903
Han, C., Park, S.-H., Kim, H.-I., & Chang, K. 2000, *MNRAS*, 316, 665
Hendry, M. A., Bryce, H. M., & Valls-Gabaud, D. 2002, *MNRAS*, 335, 539
Jaroszyński, M. 2002, *Acta Astron.*, 52, 39
Jaroszyński, M., & Mao, S. 2001, *MNRAS*, 325, 1546
Kubas, D., et al. 2005, *A&A*, 435, 941
Mao, S., & Paczyński, B. 1991, *ApJ*, 374, L37
Paczynski, B. 1986, *ApJ*, 304, 1
Rattenbury, N. J., et al. 2005, 2005, *A&A*, 439, 645
van Belle, G. T., Ciardi, D. R., Thompson, R. R., Akeson, R. L., & Lada, E. A., 2001, *ApJ*, 559, 1155
Witt, H.J. 1995, *ApJ*, 449, 42